Optical and Quantum Electronics

An investigation of 60Co gamma radiation-induced effects on the properties of nanostructured α-MoO3 for the application in optoelectronic and photonic devices

--Manuscript Draft--

Manuscript Number:	OQEL-D-18-01062R1
Full Title:	An investigation of 60Co gamma radiation-induced effects on the properties of nanostructured α-MoO3 for the application in optoelectronic and photonic devices
Article Type:	Original Research
Keywords:	Co-60 gamma radiation source; Structural properties; Optical bandgap; α-MoO3 nanoparticles; Optoelectronic and photonic devices
Corresponding Author:	Sapan Kumar Sen, M.Sc Institute of Electronics, Bangladesh Atomic Energy Commission Dhaka, BANGLADESH
Corresponding Author Secondary Information:	
Corresponding Author's Institution:	Institute of Electronics, Bangladesh Atomic Energy Commission
Corresponding Author's Secondary Institution:	
First Author:	Sapan Kumar Sen, M.Sc
First Author Secondary Information:	
Order of Authors:	Sapan Kumar Sen, M.Sc
	Manifa Noor, M.Sc
	Md. Abdullah Al Mamun, B.Sc
	M.S. Manir, M.Sc
	M. A. Matin, PhD
	M. A. Hakim, PhD
	Salahuddin Nur, PhD
	Supria Dutta, M.Sc.
Order of Authors Secondary Information:	
Funding Information:	
Abstract:	Gamma ray has sufficient energy to ionize and displace of atoms when interacts with optoelectronic and photonic devices that are placed at γ-radiation exposure environment, can be exposed to gamma radiation, resulting the alteration of the physical properties and hence the performances of devices. A Comprehensive investigation of physical properties of the semiconductor materials under the influence of gamma radiation is essential for the effective design of devices for the application in the radiation exposure environment. In this article, a potential candidate for optoelectronics and photonic devices, orthorhombic MoO3 nanoparticles with average crystallite size of 135.31 nm successfully synthesized by hydrothermal method. Then, the properties of nanoparticles exposed to low (10 kGy) and high (120 kGy) absorbed dose of γ-rays from 60Co source were characterized by XRD, FESEM, FTIR and UV-Vis-NIR spectrophotometer and effects of absorbed doses was investigated for the first time. A significant change is observed in different physical properties of α-MoO3 nanoparticles after gamma exposure. The XRD patterns reveal the average crystallite size, intensity and the degree of crystallinity decrease for low dose (10 kGy) and increases for high dose (120 kGy). The calculated average crystallite size exposed to low and high doses are 127.79 nm and 136 nm, respectively. The lattice strain and dislocation density, however, shows the opposite trend of crystallite size with absorbed doses. This result is good evident for the deterioration of crystallinity for low dose and

	improvement for high dose. The FESEM results reveal the significant effects of gamma doses on the micrographs of layered structure and on grain size. The optical studies disclose that band gap increases gradually from 2.78 eV to 2.90 eV, this behavior is associated with the reduction of electronic localized states. These results suggest that α-MoO3 nanoparticles could tolerate high doses of gamma radiation, making it a promising candidate for optoelectronic and photonic devices for γ-ray exposure environment applications.
Response to Reviewers:	Dear Dr. Yaping Zhang Thanks for your time to review the submitted document Manuscript Number: OQEL-D-18-01062, entitled " An investigation of 60Co gamma radiation-induced effects on the properties of nanostructured α-MoO3 for the application in optoelectronic and photonic devices" Optical and Quantum Electronics (OQEL), We are submitting our revised manuscript according to reviewers' comments. In the following pages, we wrote our point-by-point responses to each of the comments of the reviewers. We shall look forward to hearing from you at your earliest convenience. Sincerely, Corresponding author Sapan Kumar Sen Scientific Officer (Researcher) Institute of Electronics, Atomic Energy Research Establishment Bangladesh atomic Energy Commission, Dhaka, Bangladesh Mobile: +8801725526175 Email: sapansenphy181@gmail.com Reviewers' comments and responses: Reviewer 1 Comment 1: It is good if the authors can list the average grain size for unirradiated and irradiated samples quantitatively so that readers can easily distinguish. Response: With the humble respect to reviewer's comment, we, all authors, don't want to change this part. As it is clearly understood from XRD and FESEM parts. Comment 2: In Figure 3, why the intensity of band at ~467 cm-1 decreases after being exposed to gamma radiation? Response: A weak peak at 467 cm-1 is attributed to the Mo (2)-O (4) bonding with the water molecule and the intensity of this band decreases with increasing gamma radiation doses. This is may be due to the generation of heat after the interaction with high energetic gamma photons. Comment 3: Figure 5 needs to be improved.

	Response: Figure 5 has been improved.

An investigation of ^{60}Co gamma radiation-induced effects on the properties of nanostructured α-MoO_3 for the application in optoelectronic and photonic devices

Sapan Kumar Sen [a,*], Manifa Noor [b], Md. Abdullah Al Mamun [b], M.S. Manir [c], M. A. Matin [b], M. A. Hakim [b], Salahuddin Nur [a], Supria Dutta[d],

[a] Institute of Electronics, Atomic Energy Research Establishment, Bangladesh Atomic Energy Commission, Dhaka, Bangladesh

[b] Department of Glass & Ceramic Engineering, Bangladesh University of Engineering & Technology, Dhaka, Bangladesh

[c] Institute of Radiation and Polymer Technology, AERE, Bangladesh Atomic Energy Commission, Dhaka, Bangladesh

[d] Ministry of Education, Government of the People's Republic of Bangladesh, Dhaka, Bangladesh.

Abstract

Gamma ray has sufficient energy to ionize and displace of atoms when interacts with optoelectronic and photonic devices that are placed at γ-radiation exposure environment, can be exposed to gamma radiation, resulting the alteration of the physical properties and hence the performances of devices. A Comprehensive investigation of physical properties of the semiconductor materials under the influence of gamma radiation is essential for the effective design of devices for the application in the radiation exposure environment. In this article, a potential candidate for optoelectronics and photonic devices, orthorhombic MoO_3 nanoparticles with average crystallite size of 135.31 nm successfully synthesized by hydrothermal method. Then, the properties of nanoparticles exposed to low (10 kGy) and high (120 kGy) absorbed dose of γ-rays from ^{60}Co source were characterized by XRD, FESEM, FTIR and UV-Vis-NIR spectrophotometer and effects of absorbed doses was investigated for the first time. A significant change is observed in different physical properties of α-MoO_3 nanoparticles after gamma exposure. The XRD patterns reveal the average crystallite size, intensity and the degree of crystallinity decrease for low dose (10 kGy) and increases for high dose (120 kGy). The calculated average crystallite size exposed to low and high doses are 127.79 nm and 136 nm, respectively. The lattice strain and dislocation density, however, shows the opposite trend of crystallite size with absorbed doses. This result is good evident for the deterioration of

crystallinity for low dose and improvement for high dose. The FESEM results reveal the significant effects of gamma doses on the micrographs of layered structure and on grain size. The optical studies disclose that band gap increases gradually from 2.78 eV to 2.90 eV, this behavior is associated with the reduction of electronic localized states. These results suggest that α-MoO_3 nanoparticles could tolerate high doses of gamma radiation, making it a promising candidate for optoelectronic and photonic devices for γ-ray exposure environment applications.

Keywords: Co-60 gamma radiation source; Structural properties; Optical bandgap; α-MoO_3 nanoparticles; Optoelectronic and photonic devices.

---

*Corresponding author: E-mail: sapansenphy181@gmail.com **(Sapan Kumar Sen)**
Cell phone: +880-1725-526175, ORCID ID: 0000-0001-5086-2758

1. Introduction

The physical properties of metal oxide semiconductors (MOSs) get considerably altered when they are exposed to ionizing radiations **(Arshak and Korostynska 2006) (Nefzi et al. 2017) (Abhirami et al. 2013a) (Qindeel 2017a) (Reyhani et al. 2018a)**. Changes in physical properties can, in turn, strongly affect the performance of metal oxide semiconductor based optoelectronic and photonic devices such as LEDs, solar cells, optical dosimeters, phototransistors, optical communication devices etc. These devices experience ionizing radiations when they are used in space applications and nuclear radiation environments such as nuclear imaging, radiotherapy, military, particle accelerator-based research and nuclear power plants **(Pervez et al. 2018) (Souli et al. 2018)**. Both the space and nuclear radiation environments contain various charged/heavy particle and gamma (γ) radiations, all of which can induce ionizing effects and structural changes.

Gamma (γ) radiation is highly energetic electromagnetic waves (EM), which has the highest penetrating capability of all radiations. High energy γ-radiation is also strongly ionizing and can be obtained in the lab from two artificially derived radionuclide, Co-60 and Cs-137 isotopes **(Pervez et al. 2018) (Souli et al. 2018)**. When gamma radiation of sufficient energy interacts with semiconducting materials, it causes ionizations and/or atomic displacements leading to

crystal structural defects in the form of vacancies, defect clusters and dislocations **(Victor A.J. VAN LINT 1987) (Lai et al. 1995) (McPherson et al. 1997)**. The type/nature of these defects depends strongly on the structural properties of host materials **(Arshak and Korostynska 2006) (Arshak et al. 2005) (Pacchioni 2000)** such as atomic mass, charge, density of the host atoms, energy etc.; the fluence of incident γ-radiation and the temperature of the target material during irradiation **(Lai et al. 1995)** also plays important roles in creating the defects/damages. The presence of structural defects in semiconducting oxide materials significantly alters the density of charge carriers, optical properties **(Abhirami et al. 2013a) (Arshak et al. 2005)** and thus, seriously affects the performances of semiconductor devices. For these reasons, the investigation of γ-radiation effect on the physical properties of metal oxide semiconductors (MOSs) has become an emerging field of research in recent years.

Physical properties of metal-oxide-semiconductors (MOSs) are extremely sensitive to gamma (γ) radiation **(Tuğluoğlu 2007)**, hence sound investigation is essential for the effective design of optoelectronic and photonic devices for the application in the gamma (γ) radiation exposure environment. A number of efforts have been devoted to explore the influence of gamma radiation on the physical properties of MOS and other materials, such as tin oxides **(Tuğluoğlu 2007)(Abhirami et al. 2013a)**, TiO_2 **(Elsalamony and Ghoneim 2013)**, silicon solar cell **(Ali et al. 2013)**, $Ag_{10}Te_{90}$ **(El-fadl et al. 2007)**, ZnO **(Reyhani et al. 2018b) (Qindeel 2017a)**, silicon and silicon nitride photonic devices **(Link et al. 2017)**, arsenic selenide **(Amin et al. 2012)**, Fe-doped CdS **(Al-zahrani et al. 2015)** etc. Physical properties of the materials can be improved **(Nefzi et al. 2017) (Al-sofiany et al. 2014)** or deteriorated **(Abhirami et al. 2013b)** linearly or exponentially depending on the applied gamma (γ) dose.

Molybdenum trioxide (MoO_3) shows attractive structural, optical and electronic properties which make it a potential candidate for optoelectronic and photonic devices. MoO_3 is an n-type semiconductor with a wide band gap of 2.70 ~ 3.15 eV **(Sinaim et al. 2012) (Martins et al. 2007)**, and is considered as one of the most fascinating fundamental transition MOSs because of its numerous technological applications in the field of solar cells **(Li et al. 2017) (Simchi et al. 2013) (Girotto et al. 2011) (Mutta et al. 2016),** OLEDs **(Dagar et al. 2015)**, rechargeable Lithium ion batteries **(Zhou et al. 2010) (Kumagai and Tanno 1988)**, optoelectronics

(Cauduro et al. 2017), photochromic devices **(Ranjba et al. 2017)**, gas sensors **(Ji et al. 2016)**, super capacitors **(Prakash et al. 2018)**, and supported catalysts **(Hu et al. 2015)**.

MoO_3 has three basic structures: the thermodynamically stable orthorhombic MoO_3 phase (α-MoO_3), and two metastable phases which consist of the monoclinic MoO_3 phase (β-MoO_3) and hexagonal MoO_3 phase (h-MoO_3) **(Andersson and Magnéli 1950) (McCarron 1986)**. In α-MoO3, the molybdenum atoms coordinate six oxygen atoms to form MoO_6 octahedra, which connected by edge sharing along [001] direction to form a zigzag chain. The chains are mutually interlinked with their corners along [100] direction, resulting in a double-layer sheet, which propagate along [010] direction via Vander Waals interactions to form the layered structure of α-MoO_3 **(Zhou et al. 2003) (Ramana et al. 2009)**. Amongst of these three structures, α-MoO_3 is the most important one which shows superior chemical and physical properties due to its layered structure.

Various approaches have been focused for the preparation of nanostructured α-MoO_3 such as sol-gel method **(Dong and Dunn 1998)**, solution combustion method **(Parviz et al. 2010)**, flame synthesis technique **(Cai et al. 2011)**, vapor phase deposition method **(Zeng 1998)**, microwave plasma process **(Klinbumrung et al. 2012),** plasma enhanced chemical vapor deposition **(Kim et al. 2017)**, oil bath heating, sintering combination **(Song et al. 2012)** and so on. Here, in this report, we demonstrated a simple and low-cost hydrothermal method to synthesize crystalline α-MoO_3 nanoparticles. To the best of our knowledge, no previous efforts have been done of the effect of γ-irradiation on the physical properties of α-MoO_3 nanoparticles. Therefore, our present experiment deals for the first time with the influence of different total absorbed doses of γ-quanta irradiation on the structural, morphological, optical and functional properties of α-MoO_3 nanoparticles. These new experimental data will yield new insights to the scientific community on gamma irradiated crystalline α-MoO_3 nanoparticles for the design, development and application of optoelectronic and photonic devices.

2. Experimental details

2.1 Materials

For the hydrothermal synthesis of orthorhombic molybdenum trioxide nanoparticles, all the reagents were analytical grade, purchased from Sigma Aldrich, and used without further

purification. The reagents involved in this process were ammonium heptamolybdate tetrahydrate (AHM) ($(NH_4)_6Mo_7O_{24}.4H_2O$, as the precursor material of α-MoO_3) and concentrate nitric acid (37% HNO_3).

2.2 Synthesis of α-MoO_3 nanoparticles

2.32 g of AHM was dissolved in 10 mL of distilled water to prepare 0.2 M AHM aqueous solution and stirred vigorously with magnetic stirring for 30 min at the speed of 60 rpm at room temperature. Then, 5 mL of concentrated nitric acid was added drop wise into the solution under stirring for 15 min at room temperature. Afterwards, the as-obtained solution was heated at 90^0 C for 4 hours in a constant temperature water bath and MoO_3 precipitates were formed. The resulting MoO_3 precipitate powders were thoroughly washed for several times with distilled water and ethanol and dried in a vacuum oven at 75^0 C for 4 hours. Further, the yield powder was annealed in an electric furnace at 450^0 C temperatures for 2 hours to obtain the α-MoO_3 nanoparticles. Reaction formula of α-MoO_3 is:

$$(NH_4)_6Mo_7O_{24}.4H_2O\,(aq) + 6\,HNO_3 \xrightarrow{85^o\,C} 7MoO_3(s) + 6NH_4NO_3(aq) + 7H_2O(l)$$

2.3 Irradiation facility by ^{60}Co gamma source

A batch type Cobalt-60 (Co-60) gamma source (63.54 kCi) was used to irradiate the samples by placing the samples (α-MoO_3 nanoparticles) at about 25.4 cm distance from the source, available at Institute of Food and Radiation Biology (IFRB), Atomic Energy Research Establishment (AERE), Bangladesh Atomic Energy Commission, Dhaka, Bangladesh. As Cobalt-60 (^{60}Co) is the most common commercially used γ-source that emits two γ-ray photons of energy 1.17 MeV and 1.33 MeV, it provides approximately 579.96 Giga gamma photons per second per centimeter square surface area to the samples at room temperature **(Mortuza et al. 2018)**. The dose rate was 12.17 kGy/h. The absorbed dose was measured by the liquid phase dosimetry system (Ceric-cerous). The sample exposure time durations were such that the overall accumulated dose was 0 kGy, 10 kGy and 120 kGy.

2.4 Characterization techniques

The structural parameters of crystal of pristine and all gamma-irradiated α-MoO_3 nanoparticles were investigated by X-Ray diffractometer (model 3040-X'Pert PRO) from 5^0 to 75^0 at 2θ

position with scanning speed of 1° min^{-1} at room temperature. The X-ray powder diffraction technique was practiced with a primary beam power of 40 kV and 30 mA for CuK_α (λ=1.54056 Å) radiations. Field emission scanning electron microscope (FESEM) (Model: JEOL JSM-7600F) with accelerating voltage 5 kV was used to observe the particle surface morphology and insight of the grain structures. The Fourier transform infrared spectroscopy (FTIR) of all α-MoO_3 samples were performed in the range of 4000–400 cm^{-1}. A FTIR-ATR (Model: Perkin Elmer Spectrum Two) with KBr pellets was used to investigate the functional properties of nanostructured α-MoO_3. The optical band gap (E_g) of the nanoparticles was thus measured from diffused reflectance spectra using UV-Vis-NIR spectroscopy (Model: PerkinElmer UV-VIS-NIR Spectrometer Lambda 1050).

3. Results and discussion

3.1 Structural properties

The powder X-ray diffraction patterns of as-synthesized and gamma irradiated with absorbed doses of 10 kGy (low dose) and 120 kGy (high dose) α-MoO_3 powders are depicted in **Fig.1(a-c)**, which shows the phase and crystallinity of the α-MoO_3 nanoparticles. All the samples show a highly crystalline orthorhombic structure (α-phase) because the intensity is strong and sharp with narrow full width at half maximum (FWHM) of diffraction peaks such as (020), (110), (040), (021), (111), (060) and (002) of α-MoO_3. All XRD peaks of α-MoO_3 nanoparticles are clearly distinguishable and designates the poly-crystalline nature of the crystal structures. The acknowledged powder X-ray diffraction patterns are well indexed with the standard data card No. JCPDS-05-0508 of the pure orthorhombic phase of MoO_3 **(Wongkrua et al. 2013)**. Furthermore, no other phases of MoO_3 like monoclinic (β-MoO_3) or hexagonal (h-MoO_3) have been found in the powder diffraction patterns.

The prominent diffraction peak corresponding to (021) crystal plane positioned at 27.32° with highest intensity of unirradiated α-MoO_3 suggests the preferential orientation. The position of prominent peak (021) of irradiated of α-MoO_3 are 27.305° and 27.35° for 10 kGy and 120 kGy, respectively. For lower absorbed dose of 10 kGy, the preferential orientation (021) shifted towards a lower diffraction angle, 2θ from unirradiated sample, moreover, it shifted towards in opposite direction for higher absorbed dose of 120 kGy as shown in **Fig.1(d)**.This shifting phenomena is due to the presence of strains in the lattice structures as well as the changing

values of inter-planar spacing **(Chithambararaj et al. 2013)**. The intensity decreases for low dose due to the creation of disorders and increases for high dose, indicating good crystallinity in high absorbed dose. This intensity variation phenomena indicates that the number of planes aligned along the (021) direction increased with gamma irradiation as Co-60 gamma rays is high energy electromagnetic waves. When the radiation dose is large enough (120 kGy) the surface energy will play an important role in the crystal growth process. In this process, atoms are easy to be attracted by (021) crystal face with high surface energy and condense there, which can result in the preferential growth of (021) plane **(Choudhary and Chauhan 2016)**. The variation in the peak intensity is directly related to the degree of crystallinity whereas that in the FWHM to the crystallite size.

XRD profile gives the information to reveal micro-structural details and some structural parameters such as, lattice constants, lattice strain, crystallite size, dislocation density, etc. can be calculated from preferential orientation (021). The lattice constants for the orthorhombic MoO_3 can be estimated from the inter-planar spacing of the $\{h\ k\ l\}$ plane with the Miller indices $h\ k\ l$ by using the following equation **(Badr et al.)**

$$\frac{1}{d_{hkl}^2} = \frac{h^2}{a^2} + \frac{k^2}{b^2} + \frac{l^2}{c^2}$$

Where, d_{hkl} is the inter-planar spacing of the $\{h\ k\ l\}$ plane and a, b and c denote the lattice constants. The average crystallite size (D_v) can be determined by using the Debye- Scherrer's method **(Badr et al.)**

$$D_v = \frac{K\lambda}{\beta_{hkl} \cos\theta_{hkl}}$$

Where, D_v , λ, K , β_{hkl} and θ_{hkl} are the volume weighted average crystallite size, the wavelength of X-ray radiation ($\lambda = 1.54056$ Å for CuK_α), the shape factor and constant ($K = 0.90$), the instrumental corrected full width at half maximum height (FWHM) of the diffraction peak (in radians) located at 2θ and the Bragg angle (in degrees), respectively.

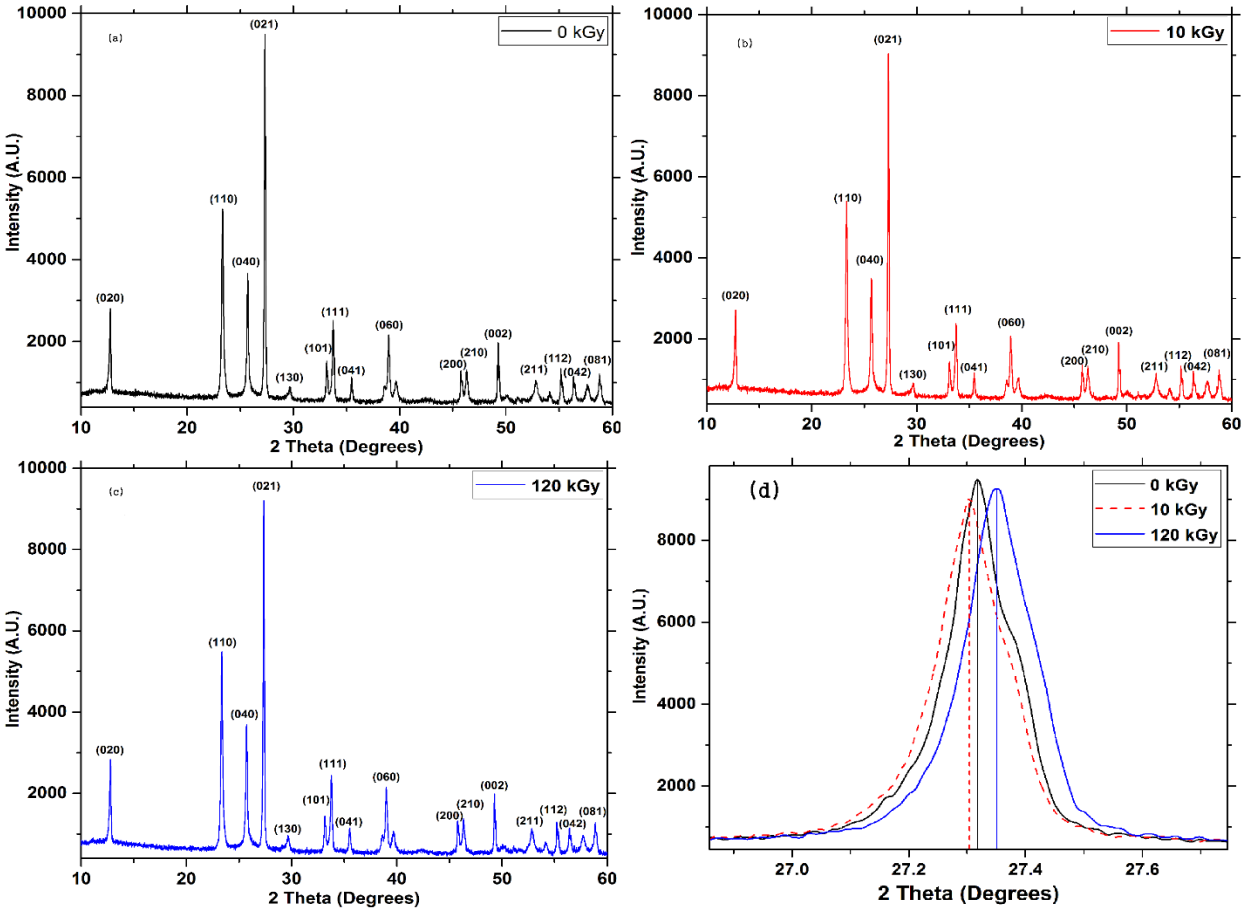

Fig. 1: XRD patterns of α-MoO_3 nanoparticles (a) unirradiated (0 kGy), (b) 10 kGy, (c) 120 kGy; (d) peak shifting, broadening and intensity variations of preferential orientation (021).

The lattice strain is responsible for the XRD line broadening which causes due to the formation of crystal defects such as imperfections and distortions **(Sivakami et al. 2016)**. The displacements of atoms with respect to reference-lattice positions, these atoms in the crystals are responsible for the formation of crystal defects **(Savaloni et al. 2006)**. The average lattice strain (ε) can be calculated by the Stokes–Wilson equation **(Chithambararaj et al. 2015)** as

$$\varepsilon = \frac{\beta_{hkl}}{4\tan\theta_{hkl}}$$

The dislocation within a nanocrystal structure refers a crystallographic defect or irregularity and mathematically it is one kind of topological defect. Many properties of a semiconductor material can be strongly affected by presence of dislocation in the crystal structure. Crystal structure in

crystalline solids is formed with the periodic arrangement of atoms or molecules on repeating fixed distance positions and this can be determined by the unit cell parameters. However, this periodic arrangement of atom or molecules in most crystalline materials is not perfect. The regular patterns are interrupted by dislocations or crystallographic defects. The movement of dislocation is impeded by other dislocations present in the sample. Thus, a larger dislocation density implies a higher hardness. The dislocation density (δ) can be determined by the following equation **(Hossain et al. 2018)**

$$\delta = 1/D_v^2$$

Where, δ and D_v are dislocation density and volume weighted average crystallite size (in nm), respectively.

Table 1: Structural Parameters of α-MoO_3 nanoparticles with different absorbed doses.

Absorbed dose (k Gy)	Lattice parameters (Å)			Crystallite size (nm)	Dislocation density ($\times 10^{-5}$ lines/m^2)	Lattice strain ($\times 10^{-4}$)
	a	b	c			
0	3.959	13.853	3.694	135.31	5.46	10.69
10	3.958	13.851	3.694	127.79	6.12	11.46
120	3.959	13.854	3.695	136.00	5.41	10.13

The calculated values of structural parameters are listed in **table 1**. It is noticed from **table 1** that, crystallite size decreases from 135.31 (pristine) to 127.79 nm for low absorbed dose (10 kGy) and then increases to 136 nm for high dose (120 kGy), indicating that the crystallinity deteriorated for low dose and improved for high dose. Whereas, lattice strain and dislocation density are changed in reverse fashion of crystallite size. At low absorbed dose (10 kGy), it appears that the crystallites of α-MoO_3 crumbling into comparatively smaller crystallites as well as yield back the amorphous material leading to the net decrease in the average crystallite size. Which is responsible for the production of crystal defects and partial amorphization of crystal structure due to the interaction with energetic gamma radiation **(Choudhary and Chauhan 2016)**. At high absorbed dose (120 kGy), however, the γ-radiation induced coalescence of small

crystallites by grain boundary collapse seem to lead to the formation of the large-sized crystallites that enhances the average crystallite size **(Sudha et al. 2016)**.

Oxygen vacancies and/or atomic displacement are produced by the interaction gamma radiation with MOSs which alters the crystal structures by increasing or decreasing defects **(Pervez et al. 2018) (Tuğluoğlu 2007) (Victor A.J. VAN LINT 1987) (Lai et al. 1995) (McPherson et al. 1997)**. Physical properties of the materials can be improved **(Nefzi et al. 2017) (Al-sofiany et al. 2014)** or deteriorated **(Abhirami et al. 2013b)** linearly or exponentially depending on the applied gamma (γ) dose. Here, due to the decreasing values of dislocation density and lattice strain which ensures the improvement of crystallinity in the region of high gamma radiation dose by decreasing the number of defects or imperfection in the crystal structures.

3.2 Surface morphology

The micrographs (×30,000) obtained by FESEM of pristine and all gamma-irradiated with doses of 10 kGy and 120 kGy of α-MoO_3 nanoparticles is shown in **Fig. 2**. FESEM micrographs are clearly indicating the formation of layered structure of orthorhombic MoO_3 nanoparticles. The properties exhibiting by the materials depend on the surface morphology of materials **(Mendelson 1969)**. It is seen from the FESEM micrographs that the microstructures are dependent on the absorbed doses of γ-radiation and it has a significant effect on the surface morphology, clearly observed from **Fig. 2**. The results indicate that the average grain sizes of the nanostructure α-MoO_3 is decreased for low dose and increased for high dose, which is good agreement with XRD results. **Fig. 2(b)** reveals the more defects formation and breaking of some grain structure for low doses due to the interaction with gamma radiation. For high dose, **Fig. 2(c)** indicates that the nanoparticles with aligned orientation and the high degree of crystallinity in the sample.

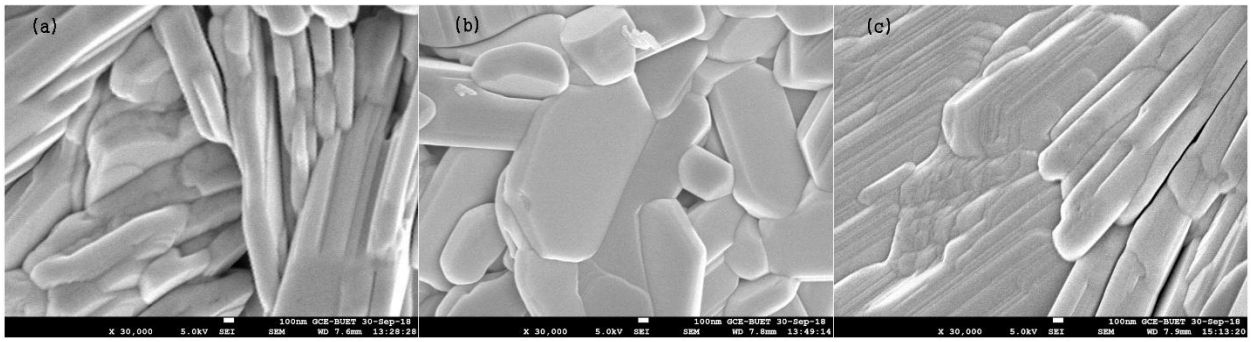

Fig. 2: FESEM images of (a) unirradiated (0 kGy) and irradiated with (b) 10 kGy (c) 120 kGy doses of α-MoO_3 nanoparticles.

3.3 Functional group analysis

The functional group of as-synthesized pristine and irradiated (10 and 120 kGy) samples of α-MoO_3 were recorded and analyzed by the FTIR spectra in the wavenumber range of 400 cm^{-1} to 4000 cm^{-1} shown in **Fig. 3**. The position, relative intensity and bandwidth of the FTIR bands of the inorganic compound dependent on the size and morphology **(Luo et al. 2009)**. The two main vibrational areas for the α-MoO_3 oxide are 1000-600 cm^{-1} and 600-400 cm^{-1}. The FTIR spectrum for pristine α-MoO_3 sample shows four strong vibrations at 563, 813, 870, and 984 cm^{-1}, respectively and variations are observed for all irradiated samples. A weak peak at 467 cm^{-1} is attributed to the Mo (2)-O (4) bonding with the water molecule and the intensity of this band decreases with increasing gamma radiation doses. This is may be due to the generation of heat after the interaction with high energetic gamma photons. The peak at 984 cm^{-1} for unirradiated α-MoO_3 sample, is attributed to the terminal Mo=O stretching vibration, indicating the layered orthorhombic MoO_3 phase **(Zakharova et al. 2007) (Chen et al. 2010) (Wongkrua et al. 2013)**, and this Mo=O stretching vibration is found for irradiated samples for doses 10 kGy, 120 kGy, at 981 cm^{-1} and 982 cm^{-1}, respectively. A strong peak at 870 cm^{-1} is assigned to the stretching vibrations of the $O_{(3)}$ atoms in the Mo-O-Mo units in orthorhombic MoO_3 structure **(Chithambararaj and Bose 2011)** and observed peak for irradiated samples with doses from 10 kGy to 120 kGy at 867 cm^{-1} , 864 cm^{-1}, respectively. The broad band at 563 cm^{-1} is due to the bending vibrations of oxygen atom ($O_{(2)}$) linked to three metal atoms $\nu(O-3Mo)$ for unirradiated α- MoO_3 sample **(Wongkrua et al. 2013)**, and similar peak can be observed for irradiated samples with doses from 10 kGy to 120 kGy at 572 cm^{-1} and 581 cm^{-1}, respectively. No water was detected in this orthorhombic-structured product. It is clear from **Fig. 3** that, absorbed dose

of gamma radiation has significant impact on stretching vibration of Mo=O and bending vibrations of Mo-O-Mo of all samples of α-MoO_3 nanoparticles which is due to the interactions of α-MoO_3 with energetic gamma radiation.

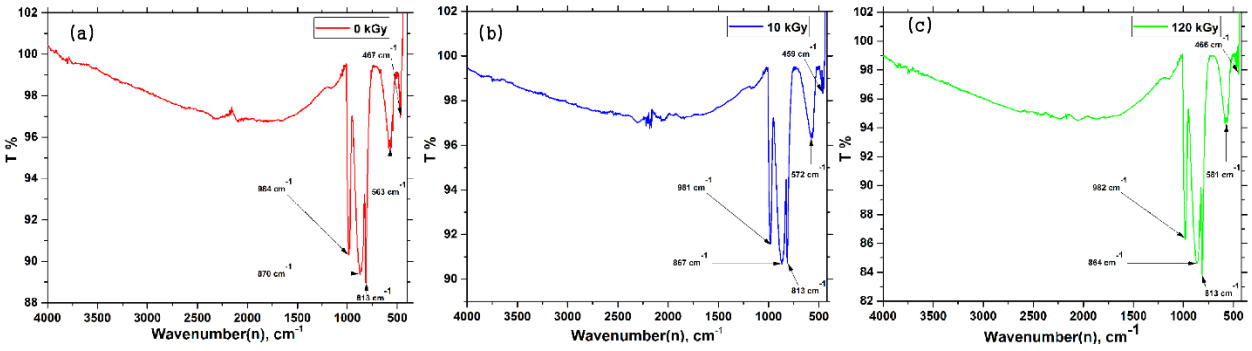

Fig. 3: FTIR spectra of unirradiated and irradiated nanostructured α-MoO_3.

3.4 Optical properties

The importance of studying the optical properties of a material is offered by the ability of this technique to provide information regarding the fundamental gap, electronic transition, trapping levels and localized states. The optical or photonic properties e.g., band gap energy of as-synthesized pristine and γ-irradiated samples were characterized by the UV-Vis NIR Spectroscopy (DRS) and the resultant spectra is shown in **Fig. 4**. The electronic band gap transition is attributed by the absorption of visible light from the top of the valence band (which is mainly composed of O 2p orbital hybridized with Mo 4d) to the bottom of the conduction band (which is mainly composed of Mo 4d orbital hybridized with O 2p) **(Chithambararaj et al. 2015)**. The optical band gap of the samples has been estimated from the Kubelka- Munk (K-M) function by employing the following equation **(Wongkrua et al. 2013)**

$$F(R) = \frac{(1-R)^n}{2R} = \frac{K(\lambda)}{S(\lambda)}$$

Further, $F(R)$ is proportional to absorption co-efficient, α i. e.,

$$F(R) \propto \alpha = \frac{\left(h\upsilon - E_g\right)^n}{h\upsilon}$$

Where, $F(R)$, R, $S(\lambda)$, h, υ, and $h\upsilon$ are the K-M function or re-emission function, the defuse reflectance of the sample, the scattering co-efficient, the Planck's constant, the photon frequency, and the incident photon energy, respectively. E_g (eV) is the energy band gap. The constant, n, known as power factor of the transition mode and the value of it varies with the variation of transition materials. The values of n for direct allowed, indirect allowed, direct forbidden and indirect forbidden transitions are 1/2, 2, 3/2 and 3, respectively. In the present case of direct transition of α-MoO_3 nanoparticles, the value of n is equal to 1⁄2. After plotting $[F(R) \times h\upsilon]^2$or $(\alpha h\upsilon)^2$ versus hν, the direct band gap of α-MoO_3 nanoparticles treated with gamma irradiation can be estimated by extrapolating the linear part of the curve as shown in **Fig. 4**. We notice that all graphs having linear parts confirm direct band gap type behavior for both non-irradiated and irradiated α-MoO_3 nanoparticles.

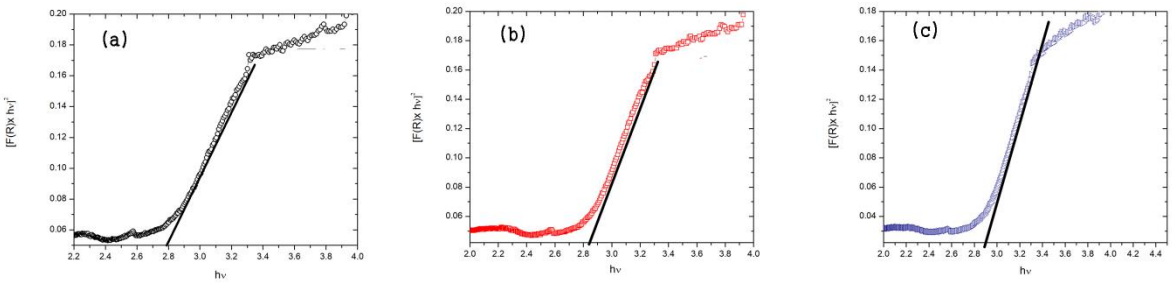

Fig. 4: Optical band gap measurement of (a) unirradiated (0 kGy) and irradiated with (b) 10 kGy (c) 120 kGy doses of α-MoO_3 nanoparticles.

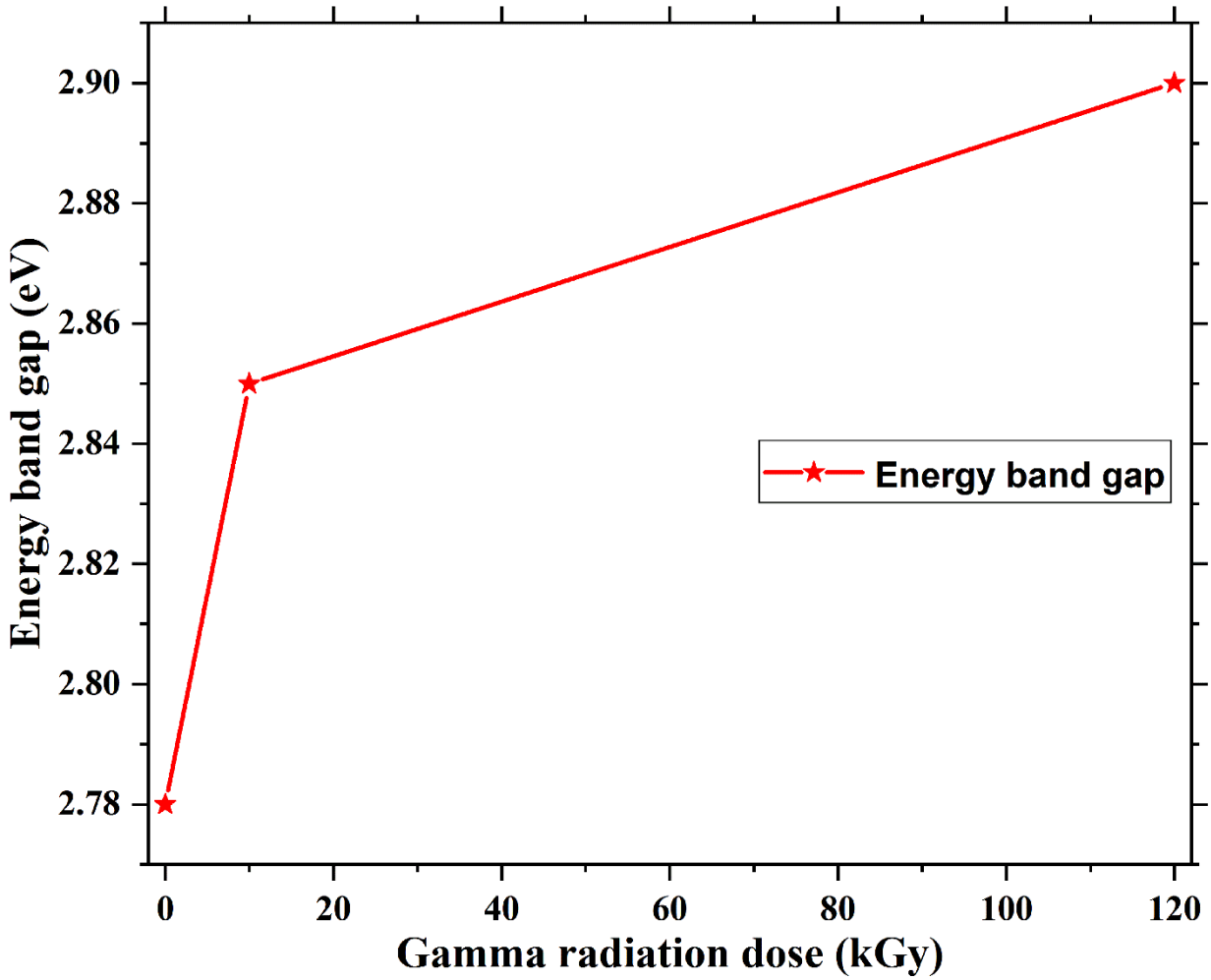

Fig. 5: Energy band gap variation of α-MoO_3 nanoparticles with different absorbed doses.

It can be noticed for non-irradiated (0 kGy) α-MoO_3, the estimated optical energy band gap is 2.78 eV (**Fig. 4a**). When α-MoO_3 nanoparticle is irradiated with low absorbed dose of gamma radiation (10 kGy), the resulting optical band gap is 2.85 eV. Furthermore, it is 2.90 eV for high dose (120 kGy). Thus, we observe that the optical band gap gradually increases from 2.78 eV to 2.90 eV with the increase of absorbed doses from 0 to 120 kGy, indicating the blue shift trend of band gap changes in a non-linear monotonic fashion with increasing absorbed doses (**Fig. 5**). which is good not only for solar cells window but other optoelectronic and photonic devices **(Qindeel 2017b)**.

Although for bulk semiconductor materials, optical band gap is constant, but it is known to vary due to particle size effects or crystallite size **(Abu EL-Fadl et al. 2007) (Shpotyuk et al. 1995)**.

The up-shifting phenomena of band gap with increasing absorbed doses may be mainly attributed due to quantum size effect and also the decrease of defects and/or structural disorders (ionization effect, displacement effect and the structure transformation induced defects) after the interaction of gamma radiation with α-MoO_3 nanoparticles. These defects and/or structural disorders produce localized states (density of defect states) in nanoparticles which increases the optical band gap **(Abu EL-Fadl et al. 2007)(Shpotyuk et al. 1995)(El-Korashy 2001)(Al-Baradi et al. 2014)(Sharma and Maity 2011)(Tripathi et al. 2015)**. Accordingly, one can expect that defects can be formed which produce localized states that change the effective Fermi level due to a decrease in carrier concentrations. This decrease in carriers in localized states will lead to an increase in the transition probabilities into the extended states, resulting the broadening in the gap **(Amin et al. 2007)**.

Furthermore, the band gap variation can also be explained according to the density of states model proposed by Mott and Davis **(Shore 2014)**. According to which, the width of the localized states near the mobility edge depends on the defects and degree of disorder present in the amorphous network structure. When the γ-rays interact with the material, induced alteration will be formed, consequently decreases the density of the localized states, which leads to decrease in the energy width of the band tails of localized states. This effect is supposed to be connected with a redistribution of the chemical bonds in the network structure. The low concentration of these localized states is responsible for the high value of optical band gap with irradiation shown in **Fig. 4**. This experimental observation strongly suggests that the irradiation significantly affects the crystallite size and hence change the optical band gap.

4. Conclusion

In summary, α-MoO_3 nanoparticles were synthesized by simplistic hydrothermal method and then irradiated with low (10 kGy) and high (120 kGy) gamma radiation doses. The effect of total absorbed dose of gamma radiation on structural, morphological and functional and optical properties of α-MoO_3 nanoparticles was investigated by spectroscopic analyses and the results showed a significant change of structural parameters, surface morphology and functional properties and bandgap after irradiation. XRD patterns reveal the crystallite size decreases from

135.31 (pristine) to 127.79 nm for low absorbed dose (10 kGy) and then increases to 136 nm for high dose (120 kGy), indicating that the crystallinity deteriorated for low dose and improved for high dose. Whereas, lattice strain and dislocation density are changed in reverse fashion of crystallite size. For lower absorbed dose of 10 kGy, the preferential orientation (021) shifted towards a lower diffraction angle, 2θ from unirradiated sample, moreover, it shifted towards in opposite direction for higher absorbed dose of 120 kGy. The intensity decreases for low dose due to the creation of disorders and increases for high dose, indicating good crystallinity in high absorbed dose. The FESEM results reveal the significant effects of gamma doses on the micrographs of layered structure and on grain size of α-MoO_3 nanoparticles.

The absorbed dose of gamma radiation has significant impact on stretching vibration of Mo=O and bending vibrations of Mo-O-Mo of α-MoO_3 nanoparticles. The optical band gap increases gradually with absorbed doses from 2.78 eV to 2.90 eV with the increase of absorbed doses from 0 to 120 kGy. These results showed that α-MoO_3 nanoparticles could tolerate high doses of gamma radiation and alters the physical properties by a marked decreasing of defects which consequences the improvement of crystallinity. This outcome makes it as a promising candidate for design, development of optoelectronic and photonic devices for space satellite and nuclear radiation exposure environment applications.

Conflict of interest

There is no conflict of interests present.

Acknowledgement

The preparation of α-MoO_3 nanoparticles and FTIR experiment were carried out at Institute of Radiation and Polymer Technology (IRPT), AERE, Bangladesh Atomic Energy Commission (BAEC), Dhaka, Bangladesh. XRD, FESEM and UV-Vis-NIR spectroscopy were conducted from Department of Glass and Ceramic Engineering, Bangladesh University of Engineering and Technology (BUET), Dhaka, Bangladesh. Gamma radiation dose was applied at GSD, IFRB, AERE, BAEC.

References

Abhirami, K.M., Sathyamoorthy, R., Asokan, K.: Structural, optical and electrical properties of gamma irradiated SnO thin films. Radiat. Phys. Chem. 91, 35–39 (2013)(a). doi:10.1016/j.radphyschem.2013.05.030

Abhirami, K.M., Sathyamoorthy, R., Asokan, K.: Structural, optical and electrical properties of gamma irradiated SnO thin films. Radiat. Phys. Chem. (2013)(b). doi:10.1016/j.radphyschem.2013.05.030

Abu EL-Fadl, A., Hafiz, M.M., Wakaad, M.M., Aashour, A.S.: Influence of γ-radiation on the

optical parameters of Ag10Te90thin films. Radiat. Phys. Chem. 76, 61–66 (2007). doi:10.1016/j.radphyschem.2006.08.007

Al-Baradi, A.M., El-Nahass, M.M., El-Raheem, M.M.A., Atta, A.A., Hassanien, A.M.: Effect of gamma irradiation on structural and optical properties of Cd_2SnO_4 thin films deposited by DC sputtering technique. Radiat. Phys. Chem. 103, 227–233 (2014). doi:10.1016/j.radphyschem.2014.05.055

Al-sofiany, S.M., Hassan, H.E., Ashour, A.H., El-raheem, M.M.A.: Study of γ-rays Enhanced Changes of the ZnO : Al Thin Film Structure and Optical Properties. Int. J. Electrochem. Sci. 9, 3209–3221 (2014)

Al-zahrani, J.H., El-hagary, M., El-taher, A.: Gamma irradiation induced effects on optical properties and single oscillator parameters of Fe-doped CdS diluted magnetic semiconductors thin films. Mater. Sci. Semicond. Process. 39, 74–78 (2015). doi:10.1016/j.mssp.2015.04.042

Ali, K., Khan, S.A., Matjafri, M.Z., Sains, U.: ^{60}Co γ -irradiation Effects on Electrical Characteristics of Monocrystalline Silicon Solar Cell. Int. J. Electrochem. Sci. 8, 7831–7841 (2013)

Amin, G.A., El-Sayed, S.M., Saad, H.M., Hafez, F.M., Abd-El-Rahman, M.: The radiation effect on optical and morphological properties of Ag-As-Te thin films. Radiat. Meas. 42, 400–406 (2007). doi:10.1016/j.radmeas.2006.12.006

Amin, G.A.M., Gregus, J., Zahoran, M.: Optical response of gamma irradiated-arsenic selenide thin films. Mater. Sci. Semicond. Process. 15, 455–459 (2012). doi:10.1016/j.mssp.2012.03.017

Andersson, G., Magnéli, A.: On the Crystal Structure of Molybdenum Trioxide., http://actachemscand.org/pdf/acta_vol_04_p0793-0797.pdf%5Cnhttp://actachemscand.org/doi/10.3891/acta.chem.scand.04-0793, (1950)

Arshak, K., Corcoran, J., Korostynska, O.: Gamma radiation sensing properties of TiO_2, ZnO, CuO and CdO thick film pn-junctions. Sensors Actuators, A Phys. 123–124, 194–198 (2005). doi:10.1016/j.sna.2005.01.014

Arshak, K., Korostynska, O.: Response of metal oxide thin film structures to radiation. Mater. Sci. Eng. B. 133, 1–7 (2006). doi:10.1016/j.mseb.2006.06.012

Badr, A.M., Elshaikh, H.A., Afify, H.H.: Hydrothermal synthesis and influence of later heat treatment on the structural evolution , optical and electrical properties of nanostructured α -MoO_3 single crystals. J. Phys. D: Appl. Phys. 50, 505111 (13pp) (2017). doi: 10.1088/1361-6463/aa97aa

Cai, L., Rao, P.M., Zheng, X.: Morphology-controlled flame synthesis of single, branched, and flower-like α-MoO_3 nanobelt arrays. Nano Lett. 11, 872–877 (2011). doi:10.1021/nl104270u

Cauduro, A.L.F., Dos Reis, R., Chen, G., Schmid, A.K., Méthivier, C., Rubahn, H.G., Bossard-Giannesini, L., Cruguel, H., Witkowski, N., Madsen, M.: Crystalline Molybdenum Oxide Thin-Films for Application as Interfacial Layers in Optoelectronic Devices. ACS Appl. Mater. Interfaces. 9, 7717–7724 (2017). doi:10.1021/acsami.6b14228

Chen, Y., Lu, C., Xu, L., Ma, Y., Hou, W., Zhu, J.J.: Single-crystalline orthorhombic molybdenum oxide nanobelts: Synthesis and photocatalytic properties. CrystEngComm. 12, 3740–3747 (2010). doi:10.1039/c000744g

Chithambararaj, A., Bose, A.C.: Hydrothermal synthesis of hexagonal and orthorhombic MoO_3 nanoparticles. J. Alloys Compd. 509, 8105–8110 (2011). doi:10.1016/j.jallcom.2011.05.067

Chithambararaj, A., Sanjini, N.S., Bose, A.C., Velmathi, S.: Flower-like hierarchical h-MoO_3: New findings of efficient visible light driven nano photocatalyst for methylene blue degradation. Catal. Sci. Technol. 3, 1405–1414 (2013). doi:10.1039/c3cy20764a

Chithambararaj, A., Winston, B., Sanjini, N.S., Velmathi, S., Bose, A.C.: Band Gap Tuning of h-MoO_3 Nanocrystals for Efficient Visible Light Photocatalytic Activity Against Methylene Blue Dye. J. Nanosci. Nanotechnol. 15, 4913–4919 (2015). doi:10.1166/jnn.2015.9846

Choudhary, R., Chauhan, R.P.: Gamma irradiation induced modifications in spin coated CdSe thin films. J. Mater. Sci. Mater. Electron. 27, 11674–11681 (2016). doi:10.1007/s10854-016-5303-x

Dagar, J., Tyagi, P., Ahmad, R., Singh, R., Sinha, O.P., Suman, C.K., Srivastava, R.: Application of 2D-MoO_3 nano-flakes in organic light emitting diodes: effect of semiconductor to metal transition with irradiation. RSC Adv. 5, 8397–8403 (2015). doi:10.1039/C4RA12430H

Dong, W., Dunn, B.: Sol–gel synthesis and characterization of molybdenum oxide gels. J. Non. Cryst. Solids. 225, 135–140 (1998). doi:10.1016/S0022-3093(98)00018-0

El-fadl, A.A., Hafiz, M.M., Wakaad, M.M., Aashour, A.S.: Influence of γ-radiation on the optical parameters of $Ag_{10}Te_{90}$ thin films. Radiat. Phys. Chem. 76, 61–66 (2007). doi:10.1016/j.radphyschem.2006.08.007

El-Korashy, A.: The effect of γ-irradiation on the optical parameters of $AgInTe_2$ Films. Radiat. Eff. Defects Solids. 153, 139–150 (2001). doi:10.1080/10420150108213266

Elsalamony, R.A., Ghoneim, S.A.: TiO2 ANATASE NANO-POWDER PREPARED BY A GAMMA RAY IRRADIATION AND PHOTOCATALYTIC ACTIVITY. 2nd International Conference on Energy Systems and Technologies. 285–293 (2013)

Girotto, C., Voroshazi, E., Cheyns, D., Heremans, P., Rand, B.P.: Solution-Processed MoO_3 Thin Films As a Hole-Injection Layer for Organic Solar Cells. ACS Appl. Mater. Interfaces. 3, 3244–3247 (2011). doi:10.1021/am200729k

Hossain, M.K., Mortuza, A.A., Sen, S.K., Basher, M.K., Ashraf, M.W., Tayyaba, S., Mia, M.N.H., Uddin, M.J.: A comparative study on the influence of pure anatase and Degussa-P25 TiO_2 nanomaterials on the structural and optical properties of DSSC photoanode. Optik (Stuttg). 171, 507–516 (2018). doi:10.1016/j.ijleo.2018.05.032

Hu, H., Deng, C., Xu, J., Zhang, K., Sun, M.: Metastable *h* -MoO $_3$ and stable α -MoO_3 microstructures: controllable synthesis, growth mechanism and their enhanced photocatalytic activity. J. Exp. Nanosci. 10, 1336–1346 (2015). doi:10.1080/17458080.2015.1012654

Ji, F., Ren, X., Zheng, X., Liu, Y., Pang, L., Jiang, J., Liu, S. (Frank): 2D-MoO_3 nanosheets for superior gas sensors. Nanoscale. 8, 8696–8703 (2016). doi:10.1039/C6NR00880A

Kim, H.-U., Son, J., Kulkarni, A., Ahn, C., Kim, K.S., Shin, D., Yeom, G.Y., Kim, T.: Highly uniform wafer-scale synthesis of α -MoO_3 by plasma enhanced chemical vapor deposition. Nanotechnology. 28, 175601 (2017). doi:10.1088/1361-6528/aa67d1

Klinbumrung, A., Thongtem, T., Thongtem, S.: Characterization of orthorhombic α-MoO_3 microplates produced by a microwave plasma process. J. Nanomater. 2012, (2012). doi:10.1155/2012/930763

Kumagai, N., Tanno, K.: Electrochemical Characteristics and Structural-Changes of Molybdenum Trioxide Hydrates As Cathode Materials for Lithium Batteries. J. Appl. Electrochem. 18, 857–862 (1988)

Lai, S.T., Alexiev, D., Nener, B.D.: Comparison between deep level defects in GaAs induced by gamma, 1 MeV electron, and neutron irradiation. J. Appl. Phys. 78, 3686–3690 (1995). doi:10.1063/1.359946

Li, Y., Yu, H., Huang, X., Wu, Z., Chen, M.: A simple synthesis method to prepare a molybdenum oxide hole-transporting layer for efficient polymer solar cells. RSC Adv. 7, 7890–7900 (2017). doi:10.1039/c7ra00303j

Link, C., Ingyang, Q.D.U., Huang, Y.I., Gbuu, O.K.O., Zhang, W.E.I., Li, J., Singh, V.I., Agarwal, A.M., Hu, J.: Gamma radiation effects in amorphous silicon and silicon nitride photonic devices. Opt. Lett. 42, 587–590 (2017). doi:https://doi.org/10.1364/OL.42.000587

Luo, H., Wei, M., Wei, K.: A new metastable phase of crystallized $MoO_3 \cdot 0.3H_2O$ nanobelts. Mater. Chem. Phys. 113, 85–90 (2009). doi:10.1016/j.matchemphys.2008.07.059

Martins, G.P., Kangsadan, T., Scott, G., Wagner, C., Van Hoose, J.: A 21st. Century Perspective on Molybdenum Powder Production by Hydrogen Reduction. Mater. Sci. Forum. 561–565, 447–452 (2007). doi:10.4028/www.scientific.net/MSF.561-565.447

McCarron, E.M.: β-MoO_3 : a metastable analogue of WO_3. J. Chem. Soc., Chem. Commun. 101, 336–338 (1986). doi:10.1039/C39860000336

McPherson, M., Jones, B.K., Sloan, T.: Effects of radiation damage in silicon p - i - n photodiodes. Semicond. Sci. Technol. 12, 1187–1194 (1997). doi:10.1088/0268-1242/12/10/003

Mendelson, M.I.: Average Grain Size in Polycrystalline Ceramics. J. Am. Ceram. Soceity. 52, 443–446 (1969). doi:https://doi.org/10.1111/j.1151-2916.1969.tb11975.x

Mortuza, M.F., Lepore, L., Khedkar, K., Thangam, S., Nahar, A., Jamil, H.M., Bandi, L., Alam, M.K.: Commissioning dosimetry and in situ dose mapping of a semi-industrial Cobalt-60 gamma-irradiation facility using Fricke and Ceric-cerous dosimetry system and comparison with Monte Carlo simulation data. Radiat. Phys. Chem. 144, 256–264 (2018). doi:10.1016/j.radphyschem.2017.08.022

Mutta, G.R., Popuri, S.R., Wilson, J.I.B., Bennett, N.S.: Sol-gel spin coated well adhered

MoO3thin films as an alternative counter electrode for dye sensitized solar cells. Solid State Sci. 61, 84–88 (2016). doi:10.1016/j.solidstatesciences.2016.08.016

Nefzi, C., Souli, M., Beji, N., Mejri, A., Kamoun-Turki, N.: Enhancement by high gamma radiations of optical and electrical properties of indium oxide thin films for solar devices. J. Mater. Sci. 52, 336–345 (2017). doi:10.1007/s10853-016-0334-5

Pacchioni, G.: Ab initio theory of point defects in oxide materials: Structure, properties, chemical reactivity. Solid State Sci. 2, 161–179 (2000). doi:10.1016/S1293-2558(00)00113-8

Parviz, D., Kazemeini, M., Rashidi, A.M., Jafari Jozani, K.: Synthesis and characterization of MoO_3 nanostructures by solution combustion method employing morphology and size control. J. Nanoparticle Res. 12, 1509–1521 (2010). doi:10.1007/s11051-009-9727-6

Pervez, M.F., Mia, M.N.H., Hossain, S., Saha, S.M.K., Ali, M.H., Sarker, P., Hossain, M.K., Matin, M.A., Hoq, M., Chowdhury, M.A.M.: Influence of total absorbed dose of gamma radiation on optical bandgap and structural properties of Mg-doped zinc oxide. Optik (Stuttg). 162, 140–150 (2018). doi:10.1016/j.ijleo.2018.02.063

Prakash, N.G., Dhananjaya, M., Narayana, A.L., Shaik, D.P., Rosaiah, P., Hussain, O.M.: High Performance One Dimensional α-MoO_3 Nanorods for Supercapacitor Applications. Ceramics International. 44, 9967-9975 (2018). doi: 10.1016/j.ceramint.2018.03.032

Qindeel, R.: Effect of gamma radiation on morphological & optical properties of ZnO nanopowder. Results Phys. 7, 807–809 (2017)(a). doi:10.1016/j.rinp.2017.02.003

Qindeel, R.: Effect of gamma radiation on morphological & optical properties of ZnO nanopowder. Results Phys. 7, 807–809 (2017)(b). doi:10.1016/J.RINP.2017.02.003

Ramana, C. V., Atuchin, V. V., Troitskaia, I.B., Gromilov, S.A., Kostrovsky, V.G., Saupe, G.B.: Low-temperature synthesis of morphology controlled metastable hexagonal molybdenum trioxide (MoO_3). Solid State Commun. 149, 6–9 (2009). doi:10.1016/j.ssc.2008.10.036

Ranjba, M., Delalat, F., Salamati, H.: Molybdenum oxide nanosheets prepared by an anodizing-exfoliation process and observation of photochromic properties. Appl. Surf. Sci. 396, 1752–1759 (2017). doi:10.1016/j.apsusc.2016.11.225

Reyhani, A., Gholizadeh, A., Khanlary, M.R.: Effect of gamma radiation on the optical and structural properties of ZnO nanowires with various diameters. Opt. Mater. (Amst). 75, 236–242 (2018)(a). doi:10.1016/j.optmat.2017.10.027

Reyhani, A., Gholizadeh, A., vahedi, V., Khanlari, M.R.: Effect of gamma radiation on the optical and structural properties of ZnO nanowires with various diameters. Opt. Mater. (Amst).75, 236-242 (2018)(b). doi:10.1016/j.optmat.2017.10.027

Savaloni, H., Gholipour-Shahraki, M., Player, M.A.: A comparison of different methods for x-ray diffraction line broadening analysis of Ti and Ag UHV deposited thin films: Nanostructural dependence on substrate temperature and film thickness. J. Phys. D. Appl. Phys. 39, 2231–2247 (2006). doi:10.1088/0022-3727/39/10/036

Sharma, S.L., Maity, T.K.: Effect of gamma radiation on electrical and optical properties of $(TeO_2)_{0·9}$ $(In_2O_3)_{0·1}$ thin films. Bull. Mater. Sci. 34, 61–69 (2011). doi:10.1007/s12034-011-0027-2

Shore, K.A.: Electronic Processes in Non-crystalline Materials (Second Edition), by N.F. Mott and E.A. Davis. Contemp. Phys. 55, 337–337 (2014). doi:10.1080/00107514.2014.933254

Shpotyuk, O.I., Matkovsky, A.O., Kovalsky, A.P., Vakiv, M.M.: Radiation-induced changes of amorphous As_2S_3 physical properties. Radiat. Eff. Defects Solids. 133, 1–4 (1995). doi:10.1080/10420159508225750

Simchi, H., McCandless, B.E., Meng, T., Boyle, J.H., Shafarman, W.N.: Characterization of reactively sputtered molybdenum oxide films for solar cell application. J. Appl. Phys. 114, 013503 (2013). doi:10.1063/1.4812587

Sinaim, H., Phuruangrat, A., Thongtem, S., Thongtem, T.: Synthesis and characterization of heteronanostructured Ag nanoparticles/MoO3nanobelts composites. Mater. Chem. Phys. 132, 358–363 (2012). doi:10.1016/j.matchemphys.2011.11.037

Sivakami, R., Dhanuskodi, S., Karvembu, R.: Estimation of lattice strain in nanocrystalline RuO_2 by Williamson – Hall and size – strain plot methods. Spectrochimica acta. Part A, Molecular and biomolecular spectroscopy. 152, 43–50 (2016). doi:10.1016/j.saa.2015.07.008

Song, L.X., Xia, J., Dang, Z., Yang, J., Wang, L.B., Chen, J.: Formation, structure and physical properties of a series of α-MoO_3 nanocrystals: from 3D to 1D and 2D. CrystEngComm. 14, 2675 (2012). doi:10.1039/c2ce06567c

Souli, M., Nefzi, C., Seboui, Z., Mejri, A., Vidu, R., Kamoun-Turki, N.: Improved structural properties, morphological and optical behaviors of sprayed Cu_2ZnSnS_4 thin films induced by high gamma radiations for solar cells. Mater. Sci. Semicond. Process. 83, 50–57 (2018). doi:10.1016/j.mssp.2018.04.009

Sudha, A., Maity, T.K., Sharma, S.L.: Effects of gamma irradiations on structural and electrical properties of indium oxide thin films prepared by thermal evaporation. Mater. Lett. 164, 372–375 (2016). doi:10.1016/j.matlet.2015.11.003

Tripathi, S.K., Kaur, J., Ridhi, R., Sharma, K., Kaur, R.: Radiation Induced Effects on Properties of Semiconducting Nanomaterials. Solid State Phenom. 239, 1–36 (2015). doi:10.4028/www.scientific.net/SSP.239.1

Tuğluoğlu, N.: ^{60}Co γ-ray irradiation effects on the interface traps density of tin oxide films of different thicknesses on n-type Si (1 1 1) substrates. Nucl. Instruments Methods Phys. Res. Sect. B Beam Interact. with Mater. Atoms. 254, 118–124 (2007). doi:10.1016/j.nimb.2006.10.082

Victor A.J. VAN LINT: The physics of radiation damage in particle detectors. Nucl. Instruments Methods Phys. Res. Sect. A Accel. Spectrometers, Detect. Assoc. Equip. 253, 453–459 (1987). doi:10.1016/0168-9002(87)90532-8

Wongkrua, P., Thongtem, T., Thongtem, S.: Synthesis of h- and α -MoO_3 by refluxing and calcination combination: Phase and morphology transformation, photocatalysis, and

photosensitization. J. Nanomater. 2013, 8 (2013). doi:10.1155/2013/702679

Zakharova, G.S., Täschner, C., Volkov, V.L., Hellmann, I., Klingeler, R., Leonhardt, A., Büchner, B.: $MoO_{3-\delta}$ nanorods: Synthesis, characterization and magnetic properties. Solid State Sci. 9, 1028–1032 (2007). doi:10.1016/j.solidstatesciences.2007.07.022

Zeng, H.C.: Chemical etching of molybdenum trioxide: A new tailor-made synthesis of MoO_3 catalysts. Inorg. Chem. 37, 1967–1973 (1998). doi:Doi 10.1021/Ic971269v

Zhou, J., Xu, N.S., Deng, S.Z., Chen, J., She, J.C., Wang, Z.L.: Large-Area Nanowire Arrays of Molybdenum and Molybdenum Oxides: Synthesis and Field Emission Properties. Adv. Mater. 15, 1835–1840 (2003). doi:10.1002/adma.200305528

Zhou, L., Yang, L., Yuan, P., Zou, J., Wu, Y., Yu, C.: α-MoO_3 Nanobelts: A High Performance Cathode Material for Lithium Ion Batteries. J. Phys. Chem. C. 114, 21868–21872 (2010). doi:10.1021/jp108778v

All Figures

An investigation of ^{60}Co gamma radiation-induced effects on the properties of nanostructured α-MoO_3 for the application in optoelectronic and photonic devices

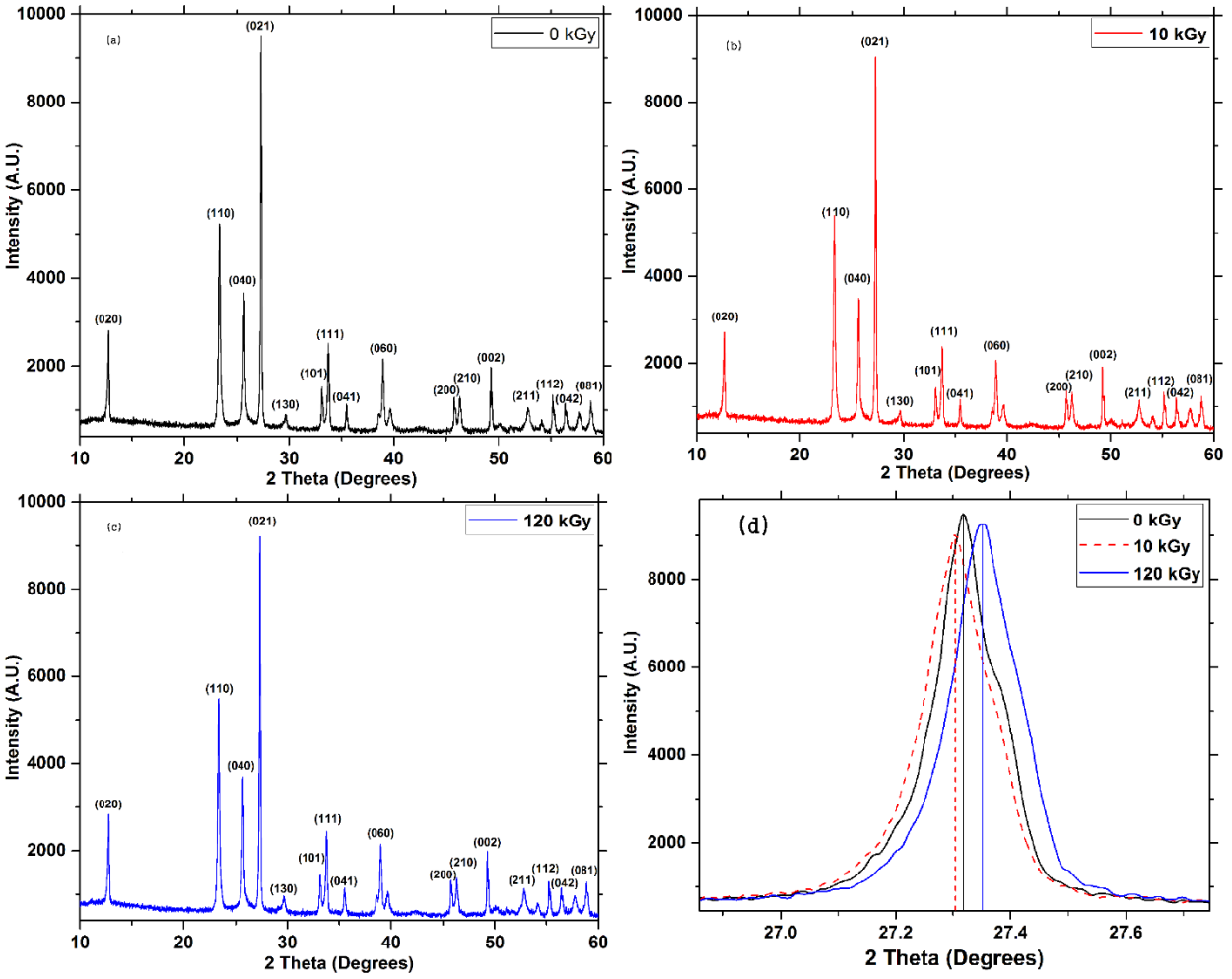

Fig. 1: XRD patterns of α-MoO_3 nanoparticles (a) unirradiated (0 kGy), (b) 10 kGy, (c) 120 kGy; (d) peak shifting, broadening and intensity variations of preferential orientation (021).

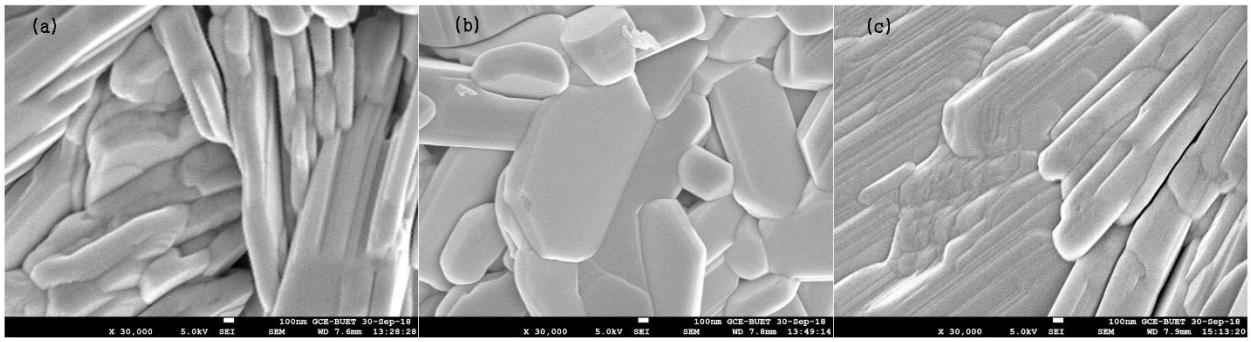

Fig. 2: FESEM images of (a) unirradiated (0 kGy) and irradiated with (b) 10 kGy (c) 120 kGy doses of α-MoO_3 nanoparticles.

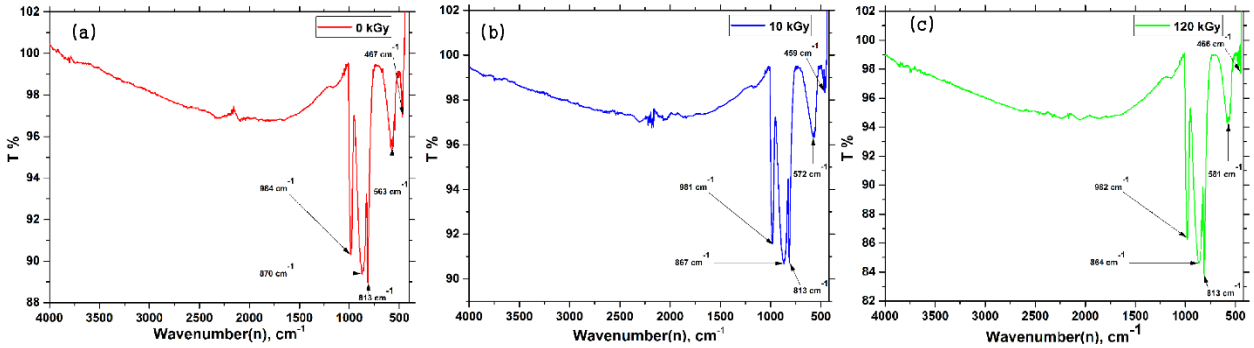

Fig. 3: FTIR spectra of unirradiated and irradiated nanostructured α-MoO_3.

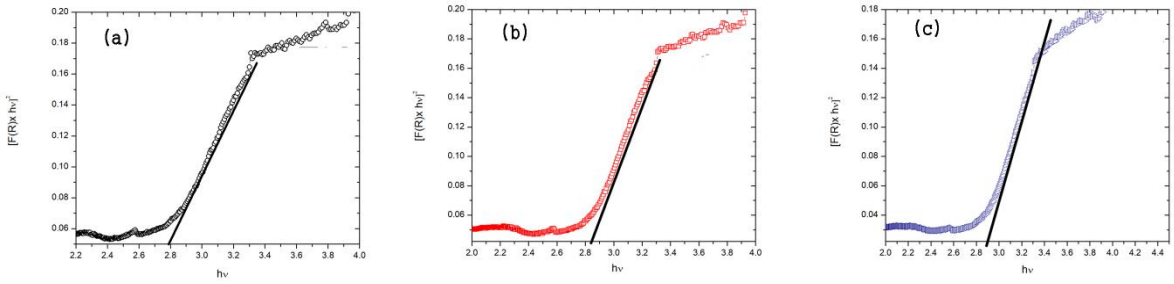

Fig. 4: Optical band gap measurement of (a) unirradiated (0 kGy) and irradiated with (b) 10 kGy (c) 120 kGy doses of α-MoO_3 nanoparticles.

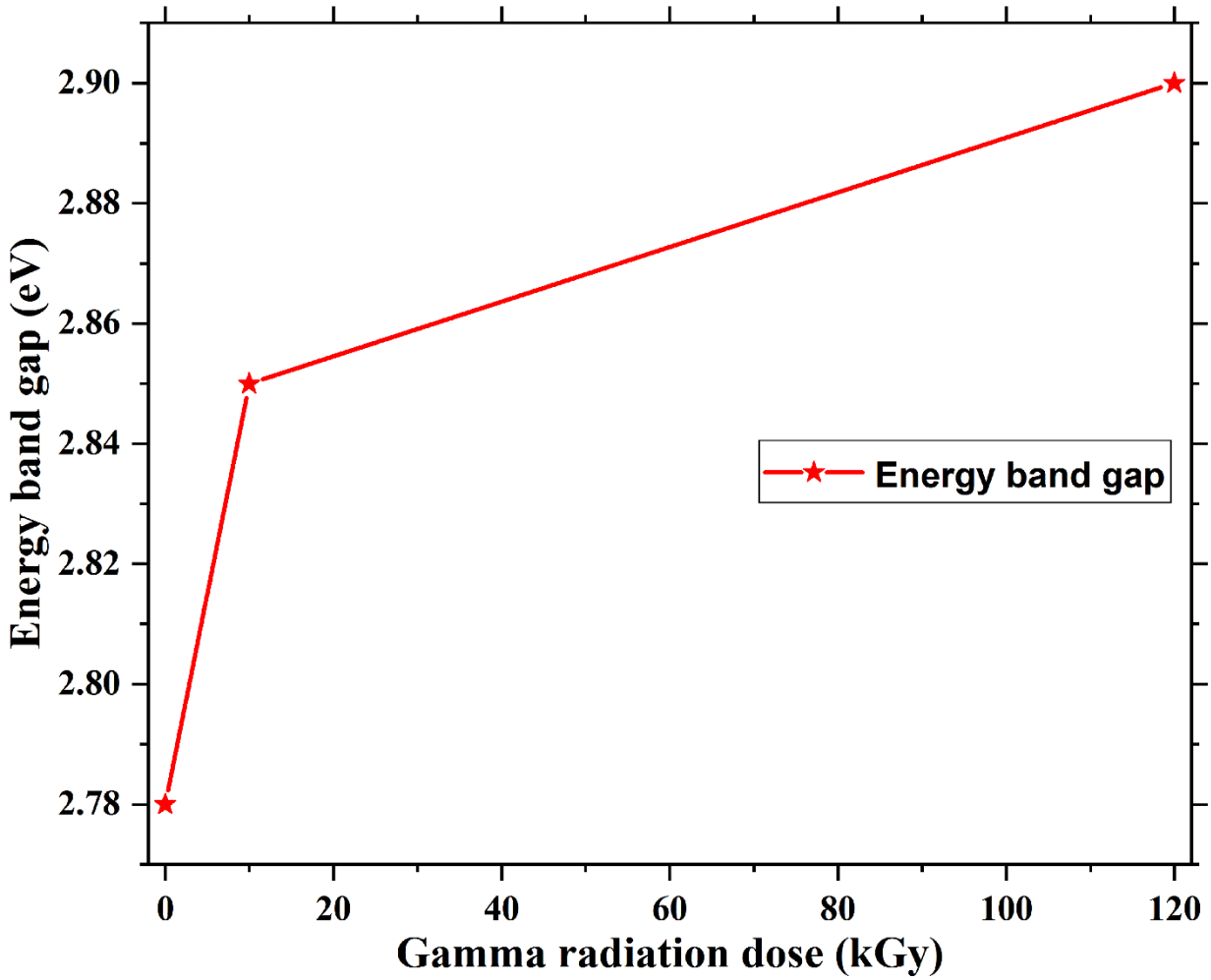

Fig. 5: Energy band gap variation of α-MoO_3 nanoparticles with different absorbed dose.